J Mater Sci (2012) 47:282–288
DOI 10.1007/s10853-011-5796-x

Composition and temperature-induced structure evolution in $Bi_{0.5}Na_{0.5}TiO_3$-based solid solutions

Feifei Wang · Min Xu · Chung Ming Leung · Yanxue Tang · Tao Wang · Xinman Chen · Wangzhou Shi

Received: 21 March 2011 / Accepted: 14 July 2011 / Published online: 13 August 2011

Abstract In this study, the temperature and composition dependence of the dielectric, ferroelectric properties, and polarization current characteristics of the $(0.935 - x)Bi_{0.5}Na_{0.5}TiO_3$–$0.065BaTiO_3$–$xSrTiO_3$ (BNBSTx) with x ranging from 0.02 to 0.22 were systematically investigated. At elevated temperature the BNBSTx solid solution with $x < 0.18$ underwent a transition from ferroelectric to short-range displacement order and then to non-polar phases. The corresponding transition temperature decreased with Sr content x increasing and the critical composition x was determined to be around 0.18–0.22. In addition, the maximum-permittivity temperature T_m, which exhibited broad peaks with nearly frequency-independent behavior, almost disappeared for $x > 0.18$, which may be related with the formation of certain sublattices in the complex solid solution.

Introduction

For half a century, the dominant piezoelectric material is the lead-oxide based, represented by the Pb(Zr, Ti)O_3 (PZT) systems which have been widely applied to various sensors, actuators, and ultrasonic transducers [1, 2]. However, due to the concerns about their toxicity, environmental legislation in the European Union [3], parts of Asia, and the US has been passed, and lead has been banned from many commercial applications such as solder and glass. This also gave a boost to the search for high performance lead-free counterparts [4]. Sodium bismuth titanate $Bi_{0.5}Na_{0.5}TiO_3$ (BNT), as one of the most promising lead-free system, has attracted continuous attention in recent years due to its high ferroelectric polarization and good piezoelectric performance [5–7]. In order to further improve its piezoelectric response and decrease its electrical conductivity, various solid solutions based on BNT has been developed such as binary system $Bi_{0.5}Na_{0.5}TiO_3$–$BaTiO_3$ [8], $Bi_{0.5}Na_{0.5}TiO_3$–$K_{0.5}Na_{0.5}NbO_3$ (BNT–KNN) [9], and $Bi_{0.5}Na_{0.5}TiO_3$–$Bi_{0.5}K_{0.5}TiO_3$ [10], ternary ones such as $Bi_{0.5}Na_{0.5}TiO_3$–$BaTiO_3$–$Bi_{0.5}K_{0.5}TiO_3$ [11], and $Bi_{0.5}Na_{0.5}TiO_3$–$BaTiO_3$–$K_{0.5}Na_{0.5}NbO_3$ (BNT–BT–KNN) [12] etc.

It is known that BNT has a complicated phase structure and with the temperature increasing, the pure BNT transforms from rhombohedral to tetragonal (T_{R-T}) phase at around 260 °C then to cubic phase (T_{T-C}) at around 540 °C [6, 7]. Moreover, there exist two other characteristic temperatures called the depolarization temperature (T_d) and the maximum-permittivity temperature (T_m). The temperature T_d, at which the piezoelectric response disappears, is quite important factor for practical applications. It is generally considered T_d corresponds to a ferroelectric to antiferroelectric phase transition due to the well-observed double hysteresis loops [13]. Recently, Kounga et al. and Zhang et al. [9, 12] reported large electric-field-induced strain value in BNT–KNN and BNT–BT–KNN solid solutions with the normalized piezoelectric constant as high as ~300 and ~560 pC/N, respectively. Zhang et al. [12] proposed the high strain response originated from the field-induced antiferroelectric (through shifting T_d to around room temperature by introducing KNN) to ferroelectric phase

F. Wang (✉) · M. Xu · Y. Tang · T. Wang · X. Chen · W. Shi
Key Laboratory of Optoelectronic Material and Device, Mathematics & Science College, Shanghai Normal University, Shanghai 200234, China
e-mail: f_f_w@sohu.com

C. M. Leung
Department of Electrical Engineering, The Hong Kong Polytechnic University, Hung Hom, Kowloon, Hong Kong

transition and the domain contributions. Through simultaneously monitoring the longitudinal and transverse strain values, Jo et al. [14] excluded this assumption and attributed the high strain response to the composition-induced non-polar phase around room temperature. However, quite recently, Eerd et al. [15] reported a phase diagram of BNT–BT system in the range of 10–470 K through Raman spectroscopy. Results indicated that with temperature increasing to above T_d, the $(1-x)$BNT–xBT with x lower than the morphotropic phase boundary (MPB) composition of 0.055 exhibited a short-range coherence (ferroelectric, instead of non-polar or antiferroelectric) with identical phase structure to that of BNT–BT with $x > 0.055$. In a word, up to present the intrinsic nature responsible for T_d is still quite controversial [16–19] and further studies on the structure evolution around T_d along with the electrical behavior are quite necessary.

In this study, a solid solution of $(0.935-x)Bi_{0.5}Na_{0.5}TiO_3$–$0.065BaTiO_3$–$xSrTiO_3$ (BNBST or BNBSTx) was designed and fabricated using a conventional solid state reaction method. The influences of Sr substitution on the temperature dependence of the dielectric properties and the phase transition characteristics were summarized. Also, the temperature- and composition-dependent polarization current density J and polarization P was measured to study the electrical behavior around T_d and the intrinsic mechanism responsible for the property evolution was also discussed.

Experimental

BNBSTx ceramics with x from 0.02 to 0.22 were prepared by a conventional solid state reaction method. For each composition, the starting materials were weighed according to the stoichiometric formula and ball milled for 6 h in ethanol. The dried slurries were calcined at 850 °C for 2 h and then ball milled again. The powders were subsequently pressed into green disks and sintered at 1200 °C for 2 h. To minimize the evaporation of the volatile elements Bi and Na, the disks were embedded in a powder of the same composition. Silver paste was coated on both sides of the sintered samples and fired at 650 °C for 0.5 h to form electrodes. The specimens for measurement of piezoelectric properties were poled in silicone oil bath with a dc field of 3–4 kV/mm for 15 min. All the electrical measurements were performed after aging for at least 24 h.

The crystal structures of the sintered ceramics were characterized by X-ray diffractometry (D8 Focus, Germany). Dielectric constant ($\varepsilon_{33}^T/\varepsilon_0$) and loss ($\tan\delta$) of the ceramics were measured using an automatic acquisition system with an impedance analyzer (Agilent HP4294A) in the temperature T range of 25–400 °C under different frequencies. The J–E curves and P–E loops, where J, P, and E denote the polarization current density, polarization, and the electric field, respectively, were measured in silicon oil with the aid of a Sawyer–Tower circuit to apply an electric field with sine waveform.

Results and discussion

Figure 1 shows the measured X-ray (XRD) patterns for the BNBSTx ceramics with x from 0.02 to 0.22 in the 2θ range of 10–80°. From Fig. 1a, all the ceramics exhibited pure perovskite structure and no second phases could be observed. In addition, the XRD patterns in the 2θ range of the 38.5–41.5° and 45–48° were measured under a slower scanning step of 0.0025° as shown in Fig. 1b, c. No obvious peak splitting can be observed for the (111) and (200) peaks, indicating the pseudocubic structure for all the compositions with small crystal lattice distortion from the cubic phase. Based on the XRD data, the lattice constant a corresponding to the pseudocubic structure was calculated shown in the inset of Fig. 1a, which increased slightly with x increasing due to larger ionic radius of Sr^{2+} than the Bi^{3+} or Na^+. For all the compositions a located around

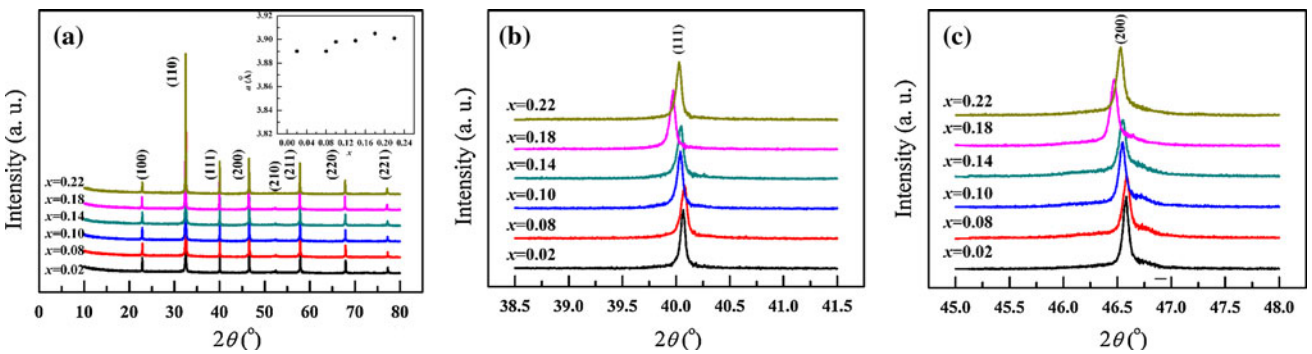

Fig. 1 The X-ray (XRD) patterns for the BNBSTx ceramics with x from 0.02 to 0.22 in the 2θ range of **a** 10–80°, **b** 38.5–41.5°, and **c** 45–48°. The *inset* shows the lattice constant as a function of the composition x

3.89–3.90 Å along with the 90°-α less than 0.05°. Besides, it should be mentioned that a discontinuity can be observed for the critical composition x of 0.18, which may be related with two phase coexistence at room temperature and will be discussed later.

Figure 2 shows the frequency and temperature dependence of the dielectric constant $\varepsilon_{33}^{T}/\varepsilon_0$ and loss tanδ of the BNBSTx ceramics with x of 0.02, 0.10, 0.18, and 0.22 from 25 to 400 °C under the frequency of 100 Hz to 100 kHz before and after poled. From all the curves, two characteristic peaks corresponding to the depolarization temperature T_d (generally determined from the loss peak in the poled ceramics indicated by the arrows) and maximum-permittivity temperature T_m can be determined and summarized in Fig. 3. With the Sr substitution increasing, both the T_d and T_m was shifted to lower temperature. In BNBST0.22, the loss peak was shifted to below room temperature and can not be observed in the experimental temperature range. For the T_m, it decreased simultaneously with x increasing, however, with the x increasing to over 0.18, an unexpected weakness was observed for the dielectric constant peaks. Such behavior has been previously observed in $Sr_{0.7}Bi_{0.2}TiO_3$–$Bi_{0.5}Na_{0.5}TiO_3$ systems [20]. This may also be correlated with the formation of certain sublattices owning ferroelectric relaxor characteristics such as $Sr_{0.7}Bi_{0.2}TiO_3$ [20].

It is well known that a typical relaxor such as $Pb(Mg_{1/3}Nb_{2/3})O_3$ (PMN) is always characterized by broad dielectric constant peaks and frequency-dependent complex susceptibility, where the $\varepsilon_{33}^{T}/\varepsilon_0$ at T_m decreases and shifts

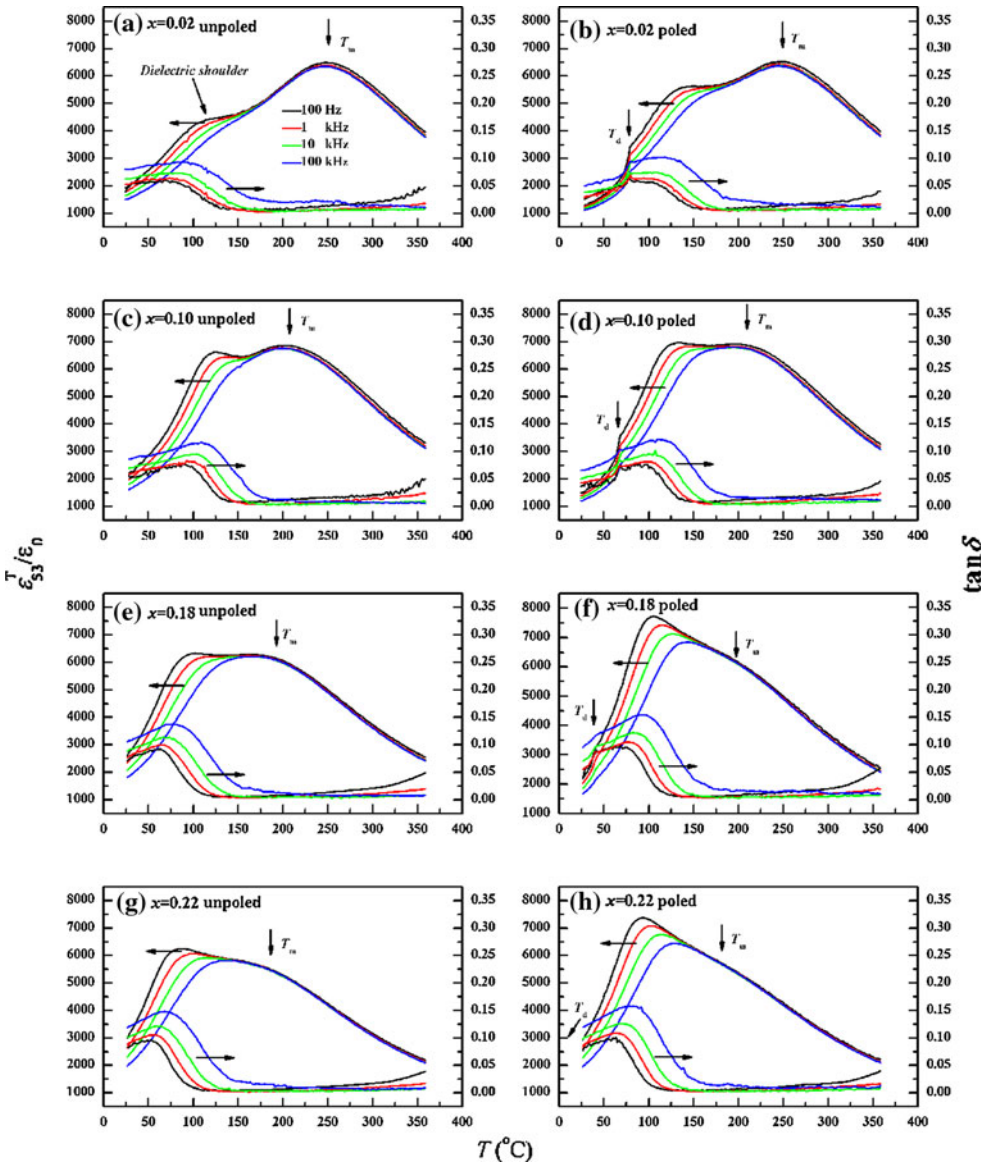

Fig. 2 The frequency and temperature dependence of the dielectric constant ($\varepsilon_{33}^{T}/\varepsilon_0$) and loss (tan$\delta$) BNBST$x$ ceramics with x of 0.02, 0.10, 0.18, and 0.22 from 25 to 400 °C under the frequency of 100 Hz to 100 kHz before and after poled

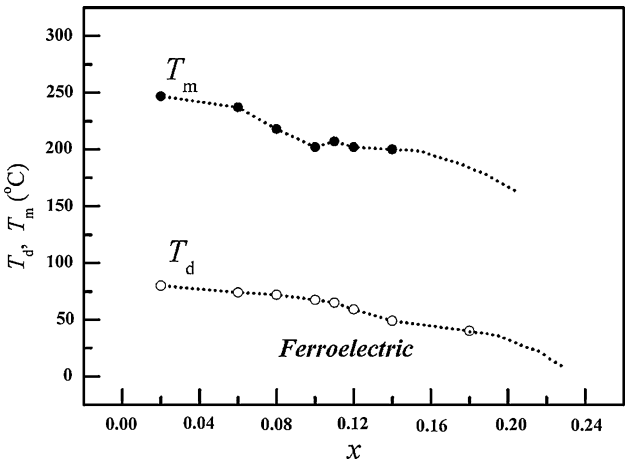

Fig. 3 Composition dependence of the depolarization temperature T_d and maximum-permittivity temperature T_m

to higher temperatures with the frequency increasing, accompanied by the frequency-dependent dielectric loss peaks with the peak temperature slightly lower than T_m [21]. In previous studies, BNT-based solid solutions were often regarded as a relaxor ferroelectric due to the broad dielectric constant peak which indicated diffused phase transition behavior [22]. From Fig. 2, broad peaks can be well observed for the BNBSTx system with $x < 0.18$. However, in BNT and the present BNBST systems, around T_m no loss peaks can be observed at all and also the dielectric constant peaks were nearly frequency-independent. The BNT-based system only exhibited diffused phase transition characteristics instead of being considered as a relaxor ferroelectric. The diffused phase transition behavior should be correlated with the multiple complexes in the A-site (such as Bi^{3+}, Na^{1+}, Ba^{2+}, Sr^{2+} etc.) of perovskite

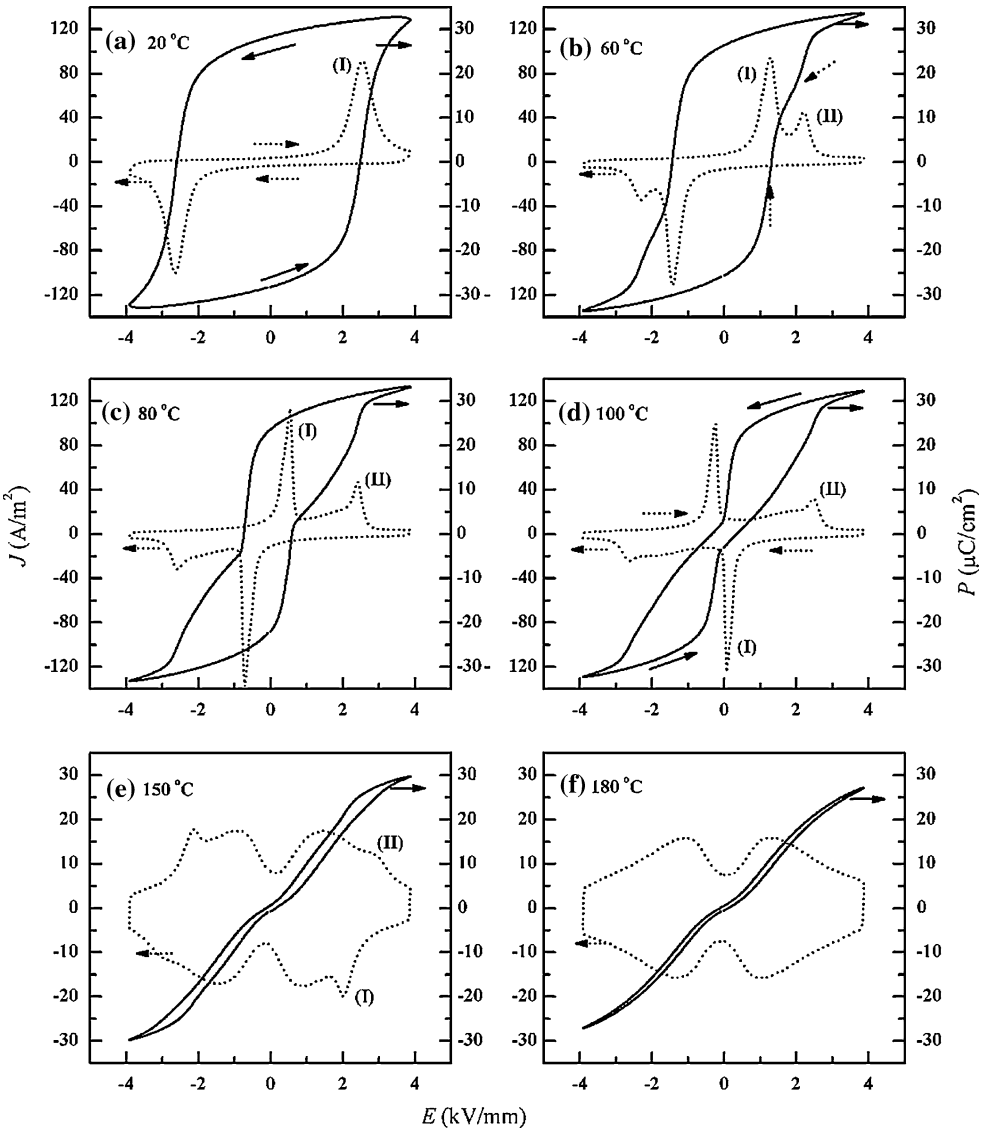

Fig. 4 Temperature dependence of polarization current density J–E curves and polarization P–E loops for BNBST0.02

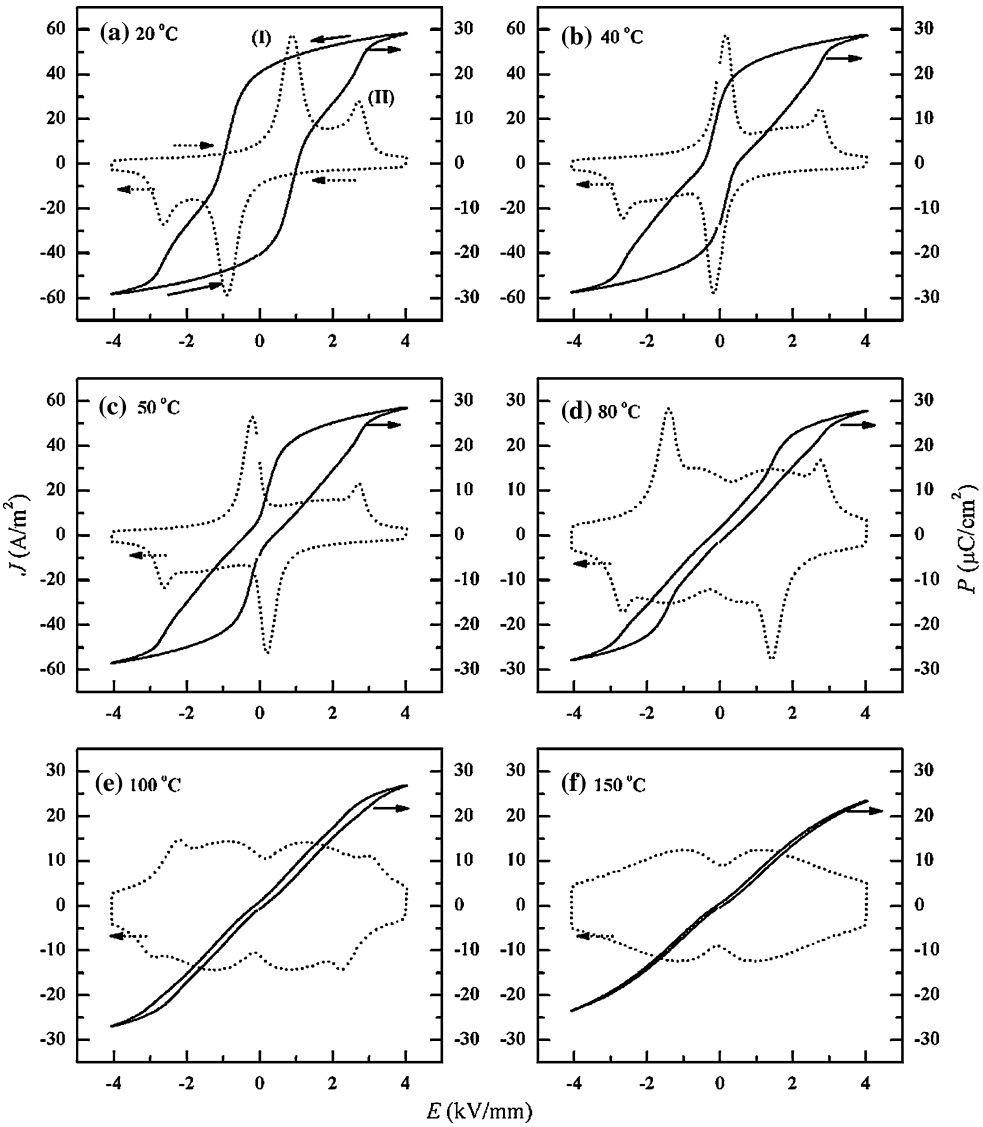

Fig. 5 Temperature dependence of polarization current density *J*–*E* curves and polarization *P*–*E* loops for BNBST0.18

compounds, which could lead to the compositional inhomogeneity in nanoscale [5]. Even though the dielectric constant peak was not that case (actually the process is complicated and still controversial up to present), we notice here the dielectric shoulder between T_d and T_m exhibits relaxor characteristics with strong frequency dispersion as shown in Fig. 2. The intrinsic nature for this also attracted much attention recently. Through Raman spectroscopy Eerd et al. [15] proposed that the phase above T_d for BNT–BT was identical to that of BNT–BT with $x > 0.055$ around room temperature, only with short-range correlation length (ferroelectric, instead of non-polar or antiferroelectric).

Here, in order to give an insight into the electrical behavior around T_d, temperature and composition dependence of polarization current density J and polarization P was investigated as shown in Figs. 4, 5, and 6 for BNBSTx with x of 0.02, 0.18, and 0.22, respectively. From Fig. 4, at 30 °C the BNBST0.02 exhibits normal rectangular *P*–*E* loop with the maximum polarization P_m, remnant polarization P_r, and coercive field E_c of 32.3 μC/cm^2, 28.3 μC/cm^2, and 2.49 kV/mm, respectively. Sharp current density peak [denoted as Peak (I)] can be observed when the applied electric field reached the E_c. At elevated temperature (60 °C), weak pinched *P*–*E* loop can be observed with E_c down to 1.31 kV/mm and Peak (I) was also simultaneously shifted to lower field direction due to easier domain motions. Besides, an unexpected small current peak [denoted as Peak (II)] appeared under the field of 2.2 kV/mm. With the temperature increased to the T_d of 80 °C, obvious pinched *P*–*E* loop can be observed and the E_c decreased close to zero. The Peak (I) was further shifted to lower field direction and the distance between Peaks (I) and (II) became larger. With the temperature T further

increased to above T_d (80 °C < T < 150 °C), Peak (II) remained unchanged while the Peak (I) appeared during the decreasing process of the field instead of ascending as shown in Fig. 4d. Simultaneously, the electric field corresponding to Peak (I) shifted to high field direction with temperature increasing in the range of 80–150 °C. Above 150 °C, both the Peaks (I) and (II) became weaker and finally disappeared at 180 °C. The *P–E* loop became very slim and exhibited pure weak double hysteresis loops with low polarization current.

The temperature-dependent variation of the *P–E* loops and *J–E* curves can be explained as follows. Near room temperature, the BNBST0.02 exhibited typical ferroelectric order with a normal hysteresis loop. The Peak (I) was originated from the ferroelectric domain switching when the field reached E_c. At elevated temperature of 60 °C, the Peak (I) was shifted downward due to easier domain motions and lower E_c. The unexpected Peak (II) appeared under high field could be considered as another kind of nature. Based on the Eerd et al.'s results [15], we suggested the unexpected Peak (II) was originated from the temperature-induced short-range ionic displacement order instead of non-polar phases suggested by Jo et al. [14], which could simultaneously explain the pinched polarization loops, large reversible strain behavior in BNT–BT–KNN system [12], the weak macroscopic piezoelectric response above T_d (the nature of non-polar phase could not explain this), and the relaxor characteristics in the dielectric spectrum between T_d and T_m shown in Fig. 2.

Furthermore, here we suggested that this short-range ionic displacement order actually appeared below T_d as evidenced by the pinched hysteresis loop at 60 °C and also the polarization current curves (Fig. 4b). With the temperature increased to T_d of 80 °C, the E_c corresponding to Peak (I) was very close to zero, however, the field corresponding to Peak (II) kept unchanged, also verifying a different nature from Peak (I). With the temperature further increased above 100 °C, in the ascending process (0–4 kV/mm), only Peak (II) remained. Peak (I) appeared during the decreasing electric field, which should be ascribed to the discharge of long-range order structures (formed during the field ascending process) upon field removal. With the temperature further increased to above 150 °C, weak Peaks (I) and (II) indicated that short-range order region decreased greatly and the external field was also difficult to set up long-range order in the ceramic. Only non-polar regions could exist at higher temperature with no frequency dispersion behavior (above 180 °C in Fig. 2a, b for BNBST0.02).

Figure 5 shows the temperature dependence of the *J–E* and *P–E* curves for BNBST0.18 which corresponds to the critical composition that pinched hysteresis hoops appeared near temperature (20 °C). Similar to those of BNBST0.02 at 60 °C, the pinched *P–E* loop exhibited much lower E_c of 1.05 kV/mm and current density Peaks (I) and (II), which indicated the coexistence of the typical ferroelectric order and the short-range coherence structure around room temperature. This indicated that the Sr substitution was favorable for the stabilization and formations of short-range ionic displacement order structure at room temperature through shifting downward the T_d (Fig. 3). With the temperature increasing, similar variation process to BNBST0.02 can be detected. Difference is that the corresponding transition temperature was shifted to lower

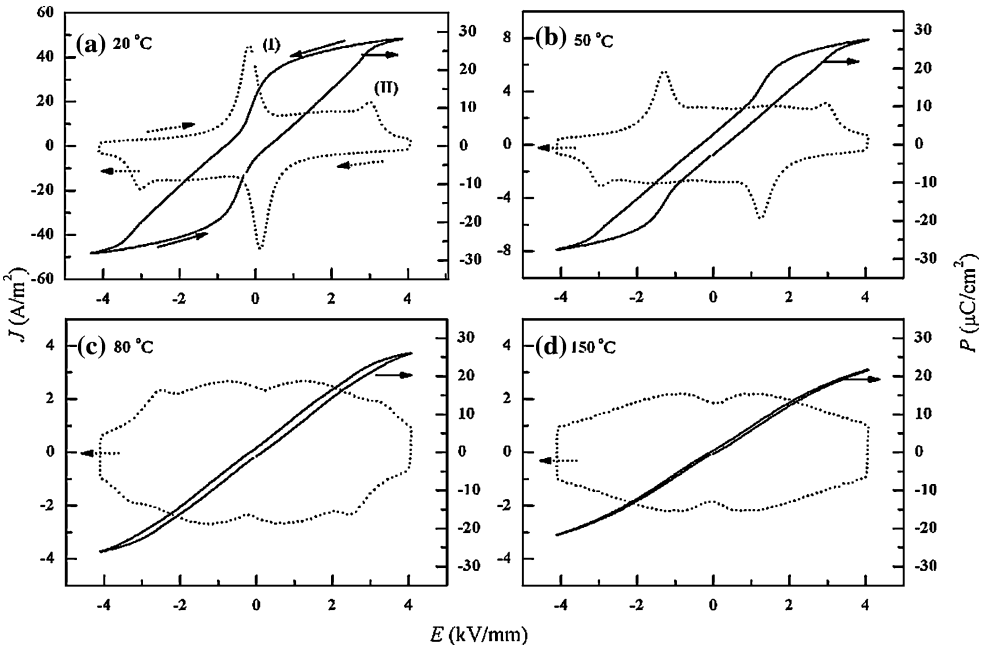

Fig. 6 Temperature dependence of polarization current density *J–E* curves and polarization *P–E* loops for BNBST0.22

temperature direction. For BNBST0.22 with the T_d below room temperature, little P_r and E_c indicated long-range ferroelectric phase could not be sustained at room temperature from the *J–E* and *P–E* curves shown in Fig. 6a. This was similar to that of BNBST0.02 at 100 °C and BNBST0.18 at 50 °C with low polarization current density and suggested the short-range coherence became the dominant structure at room temperature for high Sr substitution. In fact this was a typical composition-modulated structure evolution process. The structure discontinuity in x of 0.18 may also be related with the structure variation which corresponds to the critical composition where two phases coexisted at room temperature. The Peak (I) appeared during the field decreasing process at 20 °C meant that long-range order can still be established for BNBST0.22 ceramics under the field of 4 kV/mm.

Conclusions

In summary, the temperature and composition dependence of the dielectric and ferroelectric properties of BNBST ceramics was systematically investigated with the emphasis on the electrical behavior around T_d. With the temperature increasing, at low Sr substitution the BNBST underwent a transition from ferroelectric to short-range coherence and then to non-polar phases. The transition temperature decreased with x increasing and the critical composition x was determined to be around 0.18–0.22. This could provide important information for understanding the depolarization behavior in BNT system.

Acknowledgements This study was supported by the Science and Technology Commission of Shanghai Municipality (Grant No. 10ZR1422300 and 09520501000), the Innovation Program of Shanghai Municipal Education Commission (Grant No. 11YZ82, 11YZ83, and 11ZZ117), Shanghai Normal University Program (SK201026 and PL929), National Natural Science Foundation of China (Grant No. 60807036) and Condensed Physics of Shanghai Normal University (Grant No. DZL712).

References

1. Uchino K (1997) Piezoelectric actuators and ultrasonic motors. Kluwer, Boston
2. Jaffe B, Cook WR, Jaffe H (1971) Piezoelectric ceramics. Academic Press, London
3. Directive 2002/95/EC of the European Parliament and of the Council of 27 January 2003, Official Journal of the European Union 2003. p L37/19
4. Rödel J, Jo W, Seifert TPK, Anton EM, Granzow T, Damjanovic D (2009) J Am Ceram Soc 92:1153
5. Smolenskii GA, Isupov VA, Agranovskaya AI, Krainik NN (1961) Sov Phys Solid State (Engl Transl) 2:2651
6. Jones GO, Thomas PA (2002) Acta Crystallogr Sect B Struct Sci 58:168
7. Jones GO, Thomas PA (2000) Acta Crystallogr Sect B Struct Sci 56:426
8. Daniels JE, Jo W, Rödel J, Jones JL (2009) Appl Phys Lett 95:032904
9. Kounga AB, Zhang ST, Jo W, Granzow T, Rödel J (2008) Appl Phys Lett 92:222902
10. Royles AJ, Bell AJ, Jephcoat AP, Kleppe AK, Milne SJ, Comyn TP (2010) Appl Phys Lett 97:132909
11. Shieh J, Wu KC, Chen CS (2007) Acta Mater 55:3081
12. Zhang ST, Kounga AB, Aulbach E, Ehrenberg H, Rödel J (2007) Appl Phys Lett 91:112906
13. Takenaka T, Maruyama K, Sakata K (1991) Jpn J Appl Phys 30:2236
14. Jo W, Granzow T, Aulbach E, Rodel J, Damjanovic D (2009) J Appl Phys 105:094102
15. Eerd BW, Damjanovic D, Klein N, Setter N, Trodahl J (2010) Phys Rev B 82:104112
16. Sakata K, Masuda Y (1974) Ferroelectrics 7:347
17. Suchanicz J, Roleder K, Kania A, Handerek J (1988) Ferroelectrics 77:107
18. Isupov VA (2005) Ferroelectrics 315:123
19. Dorcet V, Trolliard G, Boullay P (2008) Chem Mater 20:5061
20. Ang C, Yu Z (2006) Adv Mater 18:103
21. Cross LE (1987) Ferroelectrics 76:241
22. Lin DM, Kwok KW, Chan HWL (2007) J Phys D Appl Phys 40:5344